

Article

Yields of Photo-Proton Reactions on Nuclei of Nickel and Separation of Cobalt Isotopes from Irradiated Targets

Andrey G. Kazakov ^{1,*}, Julia S. Babenya ¹, Taisya Y. Ekatoeva ¹, Sergey S. Belyshev ^{2,3}, Vadim V. Khankin ³, Alexander A. Kuznetsov ^{2,3}, Sergey E. Vinokurov ¹ and Boris F. Myasoedov ¹

¹ Radiochemistry Laboratory, Vernadsky Institute of Geochemistry and Analytical Chemistry, The Russian Academy of Sciences, Kosygin St., 19, 119991 Moscow, Russia; fanta2000-10@mail.ru (J.S.B.); ekatova.t@gmail.com (T.Y.E.); vinokurov.geokhi@gmail.com (S.E.V.); bfmyas@mail.ru (B.F.M.)

² Department of Physics, Lomonosov Moscow State University, Leninskie Gory, 1, Bld. 2, 119991 Moscow, Russia; belyshev@depni.sinp.msu.ru (S.S.B.); kuznets@depni.sinp.msu.ru (A.A.K.)

³ Skobel'syn Institute of Nuclear Physics, Lomonosov Moscow State University, Leninskie Gory, 1, Bld. 2, 119991 Moscow, Russia; v-k32@yandex.ru

* Correspondence: adeptak92@mail.ru

Abstract: Nowadays, cobalt isotopes ⁵⁵Co, ⁵⁷Co, and ^{58m}Co are considered to be promising radionuclides in nuclear medicine, with ⁵⁵Co receiving the most attention as an isotope for diagnostics by positron emission tomography. One of the current research directions is dedicated to its production using electron accelerators (via photonuclear method). In our work, the yields of nuclear reactions occurring during the irradiation of ^{nat}Ni and ⁶⁰Ni by bremsstrahlung photons with energy up to 55 MeV were determined. A method of fast and simple cobalt isotopes separation from irradiated targets using extraction chromatography was developed.

Keywords: photonuclear method; cobalt isotopes; cobalt-55; extraction chromatography; nuclear medicine



Citation: Kazakov, A.G.; Babenya, J.S.; Ekatoeva, T.Y.; Belyshev, S.S.; Khankin, V.V.; Kuznetsov, A.A.; Vinokurov, S.E.; Myasoedov, B.F. Yields of Photo-Proton Reactions on Nuclei of Nickel and Separation of Cobalt Isotopes from Irradiated Targets. *Molecules* **2022**, *27*, 1524.

<https://doi.org/10.3390/molecules27051524>

Academic Editors: Alessandra Boschi and Petra Martini

Received: 25 January 2022

Accepted: 21 February 2022

Published: 24 February 2022

Publisher's Note: MDPI stays neutral with regard to jurisdictional claims in published maps and institutional affiliations.



Copyright: © 2022 by the authors. Licensee MDPI, Basel, Switzerland. This article is an open access article distributed under the terms and conditions of the Creative Commons Attribution (CC BY) license (<https://creativecommons.org/licenses/by/4.0/>).

1. Introduction

Two main methods for producing radioisotopes or their generators for nuclear medicine are widely used today: in nuclear reactors and cyclotrons. Another possible way of their production is photonuclear method. Production of radioactive isotopes for different purposes by this method was widely investigated in the 1970–1980s, and today the growing number of studies on medical isotopes production by photonuclear method can be observed. Due to the development of this method, nowadays ⁴⁷Sc, ⁶⁷Cu, and ^{99m}Tc generator as well as light isotopes ¹¹C, ¹³N, ¹⁵O, ¹⁸F for positron emission tomography (PET) are already obtained in electron accelerators on a regular basis, and the production of ²²⁵Ac, ¹⁷⁷Lu, ¹¹¹In, ¹⁰⁵Rh, and ⁴⁴Ti/⁴⁴Sc generator is currently being investigated [1].

Radioactive isotopes ⁵⁵Co, ⁵⁷Co, and ^{58m}Co are considered to be used in nuclear medicine, as they are not too well known and well-studied but are promising. The most attention is paid to ⁵⁵Co ($T_{1/2} = 17.5$ h, 77% β^+ , $E_{\max\beta^+} = 1498$ keV), which is auspicious for studying slow processes in an organism by PET. At the dawn of nuclear medicine, it was reported that ⁵⁵Co complexes could be used for the diagnostics of lung cancer and for the visualization of tumors [2–4]. It was shown in contemporary studies that ⁵⁵Co-EDTA is suitable for use in nephrological research [5] and for the visualization of prostate cancer [6] as well as for the detection of distant metastasis in close vicinity of the bladder and kidneys [7]. It is important to mention that the chemical properties of ⁵⁵Co(II) and its behavior in an organism are similar to that of PET-isotope ⁶⁴Cu(II) ($T_{1/2} = 12.7$ h, 17.4% β^+ , $E_{\max\beta^+} = 653$ keV) and also of Ca(II), the latter being present in body but lacking suitable radioactive isotopes for its visualization [8–10]. In comparison to ⁶⁴Cu(II), ⁵⁵Co has the following advantages: first, compounds labeled with ⁵⁵Co tend to be absorbed less by the

liver than compounds labeled with ^{64}Cu . Second, the higher yield of positrons produced by ^{55}Co results in less activity of the drug and/or less time required for PET diagnostics. Using ^{55}Co in PET as an indicator of calcium allows one to visualize the affected tissue in patients with traumatic brain injury and to estimate neuronal damage with strokes and brain tumors [11–13]. As for other medical isotopes of Co, $^{58\text{m}}\text{Co}$ ($T_{1/2} = 9.04$ h) is Auger emitter and thus is suitable for Auger therapy, and ^{57}Co ($T_{1/2} = 271.8$ d, $E_{\gamma} = 122$ keV) is suitable for preclinical research and the study of pharmacokinetics of drugs based on cobalt due to the long half-life of this isotope and the high yield of produced gamma-quanta [14].

In spite of the advantages listed above, the use of cobalt isotopes in medicine is limited by the difficulties of their production (Figure 1). ^{55}Co is mainly produced in cyclotrons by nuclear reactions $^{54}\text{Fe}(d,n)^{55}\text{Co}$, $^{56}\text{Fe}(p,2n)^{55}\text{Co}$, and $^{58}\text{Ni}(p,\alpha)^{55}\text{Co}$ [15]. However, all listed ways of production require enriched targets, which would also prevent long-lived radioactive impurities ^{56}Co ($T_{1/2} = 77.27$ d) and ^{57}Co from forming [16]. According to calculations, when a target made of 100% ^{54}Fe is irradiated with deuterons, a yield of up to 30 MBq/ $\mu\text{A}\cdot\text{h}$ can be achieved, while the content of long-lived cobalt isotopes is minimal [15]. In the case of irradiation of 100% ^{56}Fe with protons, a significantly higher yield can be achieved up to 180 MBq/ $\mu\text{A}\cdot\text{h}$; however, the content of ^{56}Co will also be higher. Finally, for the $^{58}\text{Ni}(p,\alpha)^{55}\text{Co}$ reaction using an enriched target, the maximum yield is 13 MBq/ $\mu\text{A}\cdot\text{h}$, and the impurity content is minimal. Thus, $^{54}\text{Fe}(d,n)^{55}\text{Co}$ is the most promising reaction for use in nuclear medicine among cyclotron ones.

^{55}Ni 204.7 ms	^{56}Ni 6.1 d	^{57}Ni 35.6 h	^{58}Ni stable 68.1 %	^{59}Ni $7.6\cdot 10^4$ y	^{60}Ni stable 26.2 %
^{54}Co 193.3 ms	^{55}Co 17.5 h	^{56}Co 77.2 d	^{57}Co 271.7 d	^{58}Co 70.9 d	^{59}Co stable 100 %
^{53}Fe 8.5 min	^{54}Fe stable 5.9 %	^{55}Fe 2.7 y	^{56}Fe stable 91.8 %	^{57}Fe stable 2.1 %	^{58}Fe stable 0.3 %

(1) $^{54}\text{Fe}(d,n)^{55}\text{Co}$
 (2) $^{56}\text{Fe}(p,2n)^{55}\text{Co}$
 (3) $^{58}\text{Ni}(p,\alpha)^{55}\text{Co}$
 (4) $^{58}\text{Ni}(\gamma,p2n)^{55}\text{Co}$
 (5) $^{60}\text{Ni}(\gamma,p4n)^{55}\text{Co}$

Figure 1. Studied methods of ^{55}Co production.

Cobalt isotopes (including ^{55}Co) can also be obtained using an electron accelerator—by irradiation of nickel. Currently, data on yields of photo-proton reactions on nickel nuclei, leading to the formation of medical isotopes of cobalt, is limited. In works [17,18], flux-weighted average cross-sections of reactions $^{\text{nat}}\text{Ni}(\gamma,pxn)$ in energy range of 55 to 75 MeV were determined. It was established that cross-sections of $^{\text{nat}}\text{Ni}(\gamma,pxn)^{55}\text{Co}$ in this range varied insignificantly. However, there are no data on the yields of nuclear reactions in these works, which makes it impossible to evaluate the possibility of obtaining cobalt isotopes in sufficient quantities for nuclear medicine using electron accelerators.

No methods of separation of cobalt isotopes produced in an electron accelerator can be found in the literature. At the same time, there are works dedicated to the separation of cobalt isotopes from cyclotron-irradiated nickel targets. In these works, Ni(II) and Co(II) were separated using anion exchange resin Dowex AG-1X8 [11,14,19–27] and using extraction chromatography sorbent based on diglycolamide, where Co(II) was obtained in 3 M HCl [28]. The best results were achieved in the last case, the yield of cobalt was 92%, separation factors of cobalt from different impurities varied from $8\cdot 10^2$ to $2\cdot 10^4$, and the process lasted for 2 h. It is worth mentioning that the main task of these works was more difficult than just separation of cobalt and nickel: first, irradiation of nickel also results in the formation of copper isotopes; second, nickel was usually applied via electrodeposition as a coating to a metal plate, irradiation of which also led to impurities. To produce cobalt isotopes for nuclear medicine purposes, it is necessary to develop a technique with higher

yield, higher Ni/Co separation factors, and less time of separation, allowing one to obtain cobalt in diluted HCl medium.

Thus, the purpose of this work was to determine yields of photonuclear reactions on nickel nuclei and also to develop a fast, simple, and effective method of carrier-free cobalt isotopes separation from nickel targets.

2. Results and Discussion

2.1. Radionuclide Composition of Irradiated Targets and Yields of Nuclear Reactions

Gamma-spectra of irradiated targets made of ^{nat}Ni and ^{60}Ni are presented in Figure 2A,B; yields of photonuclear reactions leading to the formation of nickel and cobalt isotopes during the irradiation of ^{nat}Ni , ^{60}Ni , and ^{58}Ni are presented in Table 1. It was established that in each case, ^{55}Co was produced along with significant quantities of long-lived impurities $^{56,57,58}\text{Co}$. Irradiation of ^{nat}Ni and ^{58}Ni resulted in the yield of $^{56,57,58}\text{Co}$ being 1.2–1.5 times higher than the yield of ^{55}Co , and the irradiation of ^{60}Ni led to the yield of ^{55}Co being no more than 3% of the yield of all cobalt isotopes. Obviously, ^{55}Co with such low radionuclide purity is not suitable for PET. On the other hand, isotopes $^{56,57,58}\text{Co}$ are gamma-emitters and can be used in preclinical research of radiopharmaceuticals based on cobalt, including in vivo experiments. For these purposes, we recommend irradiating ^{nat}Ni ; in this case, the yield of ^{57}Co is 66 kBq/($\mu\text{A}\cdot\text{h}\cdot\text{g}/\text{cm}^2$) on a thin plate, and this value can be increased by using massive target. ^{58}Ni can also be used as a target material increasing the yield of ^{57}Co up to 82 kBq/($\mu\text{A}\cdot\text{h}\cdot\text{g}/\text{cm}^2$) on thin foil; however, targets made of ^{58}Ni are more expensive than ones made of ^{nat}Ni . Therefore, photonuclear method allows one to produce cobalt isotopes with sufficient activity for preclinical research.

Table 1. Yields of photonuclear reactions on ^{nat}Ni , ^{60}Ni (obtained experimentally), and ^{58}Ni (calculated using yields on ^{nat}Ni , ^{60}Ni nuclei) with maximum energy of bremsstrahlung photons being 55 MeV. Values obtained by TALYS [29] are presented in brackets.

Isotope	$T_{1/2}$	$Y_{\text{EOB}}, \text{kBq}/(\mu\text{A}\cdot\text{h}\cdot\text{g}/\text{cm}^2)$		
		^{nat}Ni	^{60}Ni	^{58}Ni
^{56}Ni	6.08 d	20.7 ± 0.3 (32.5)	0.16 ± 0.01 (0.06)	29.6 ± 0.3 (47.7)
^{57}Ni	35.6 h	3883 ± 76 (4404)	48.3 ± 1.0 (21)	5440 ± 93 (6460)
^{55}Co	17.53 h	60.2 ± 4.2 (72.9)	1.1 ± 0.1 (0.02)	82.4 ± 5.1 (107)
^{56}Co	77.27 d	16.5 ± 0.1 (17.4)	0.48 ± 0.03 (0.16)	21.6 ± 0.2 (25.4)
^{57}Co	271.8 d	66.1 ± 0.4 (46.5)	2.75 ± 0.04 (1.35)	81.8 ± 0.6 (67.8)
^{58}Co	70.86 d	10.3 ± 0.1 (3.6)	39.6 ± 0.4 (13.6)	0

Table 1 also compares the experimentally measured yields with theoretical calculations using the TALYS program, taking into account the bremsstrahlung spectrum. On the whole, we can see a satisfactory agreement between the experimental yields and the theoretical calculations. The difference in values can be due to two main factors: TALYS uses default photoabsorption cross-sections, and also does not take into account the isospin splitting of the giant dipole resonance, which has a significant effect on the yields of photo-proton reactions.

2.2. Separation of Co(II) Isotopes without a Carrier Using Extraction Chromatography

Obtained chromatograms of Ni(II) and Co(II) separation using DGA resin are presented in Figure 3. It was established that elution of Co(II) by HCl solutions with concentration varying from 0.01 to 3 M resulted in similar elution profiles; yield of Co(II) was close to quantitative in each case, and the process lasted for no longer than 0.5 h. To determine the separation factor of Ni(II) and Co(II), fractions marked in Figure 3 were selected for gamma-spectra registration for 24 h. Peaks of isotopes $^{56,57}\text{Ni}$ were absent in registered gamma-spectra, and the separation factor of Ni/Co was calculated using detection limit of these radionuclides and was $2.8\cdot 10^5$, which is one order of magnitude higher than the

factor during the separation using sorbent with similar composition in work [28]. Thus, the method of carrier-free Co(II) separation was developed; it allows one to obtain necessary isotopes in different solutions of HCl, including the solutions with low concentration, which is preferable for nuclear medicine.

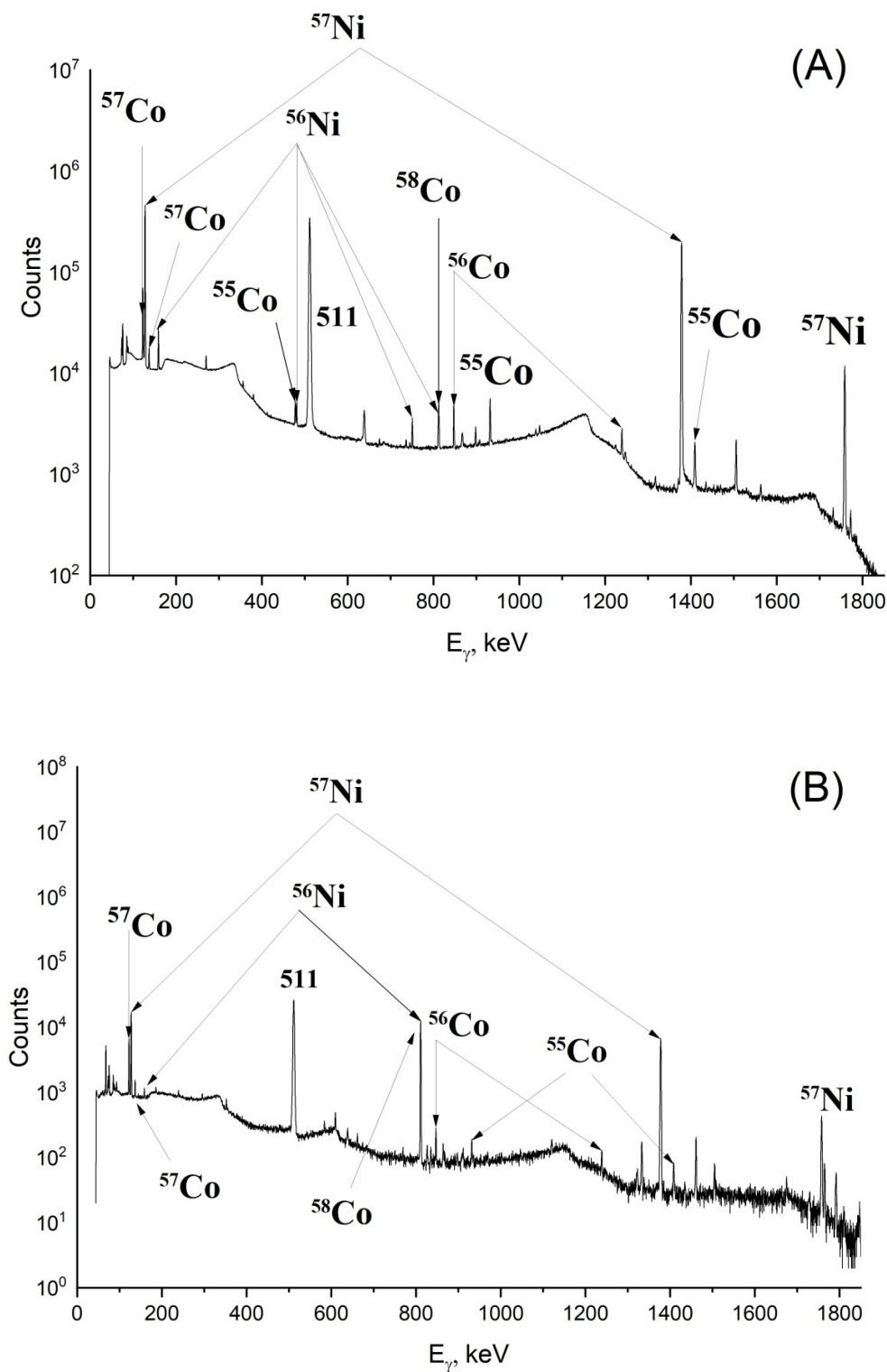


Figure 2. Gamma-spectra of ^{nat}Ni irradiated by bremsstrahlung photons with energy up to 55 MeV during 1 h after EOB (A), and of irradiated ⁶⁰Ni for 19 h after EOB (B). The most intense peaks of each isotope are labeled in the figures.

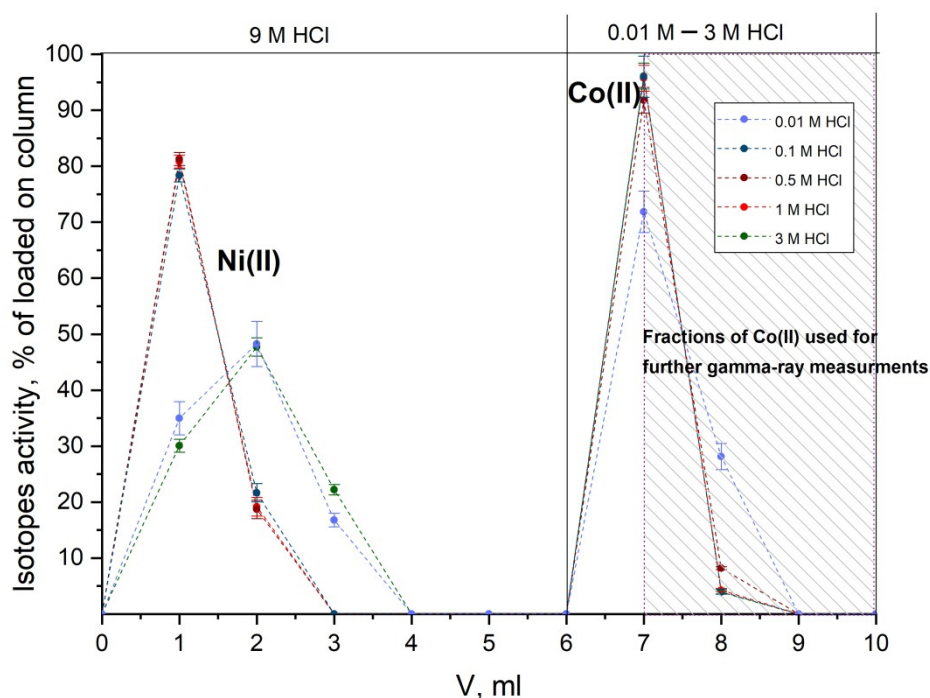


Figure 3. Elution curves of Ni(II) and Co(II) during separation on DGA resin column in HCl solutions.

As stated above in Section 2.1, the highest yields of cobalt isotopes are achieved during the irradiation of enriched ^{58}Ni targets. Obviously, the expensive target material should be regenerated after separation. For this purpose, it is possible to evaporate eluate-containing Ni(II) to dryness to irradiate NiCl_2 to produce cobalt isotopes one more time. In this case, there will be no need to dissolve the target during prolonged heating, since NiCl_2 is water-soluble. Another possible way is the irradiation of Ni(II) solution separated from the column, which can be eluted through the column again without any preparative treatment. In any case, the regeneration of enriched nickel is not complicated. It is also worth noting that formed isotopes of cobalt have $T_{1/2}$ no longer than 272 d, allowing one to utilize samples with general waste after prolonged storage, i.e., no radioactive waste requiring special treatment and disposal is produced after the irradiation. Thus, this studied method of production and separation of cobalt isotopes is environmentally friendly due to the regeneration of the target and the absence of radioactive waste.

3. Materials and Methods

3.1. Theoretical Calculations of Cross-Sections and Yields of Photonuclear Reactions

The cross-sections were calculated using the TALYS program, while the total photoabsorption cross-section was calculated based on the parameters from the RIPL-2 experimental database [30]. To calculate the cross-sections for photonuclear reactions, TALYS uses a combination of the evaporative and exciton preequilibrium decay mechanism of a compound nucleus with the emission of nucleons and gamma-quanta. The obtained cross-sections of the main photonuclear reactions leading to the formation of $^{55,56,57,58}\text{Co}$ and $^{55,56,57}\text{Ni}$ isotopes are shown in Figure 4.

The theoretical yield of isotope formation, taking into account all possible reactions leading to the formation of the selected isotope, was calculated by Equation (1):

$$Y = \frac{\lambda\alpha}{\rho q_e} \sum_i \eta_i \int_{E_i}^{E_m} \phi(E_\gamma, E_m) \sigma_i(E_\gamma) dE_\gamma \quad (1)$$

where λ is the decay constant, α is the number of studied nuclei per 1 cm^2 of target, ρ is the surface density of the target, q_e is the electron charge in $\mu\text{A}\cdot\text{h}$, index i corresponds

to the number of the reaction contributing to the formation of studied isotope, η_i is the percentage of the nickel isotope on which the reaction occurs in a natural mixture of isotopes, E_i is the threshold of the corresponding reaction, E_m is the maximum energy of the bremsstrahlung spectrum, $\sigma_i(E_\gamma)$ is the cross-section of the corresponding photonuclear reaction, and $\phi(E_\gamma, E_m)$ is the bremsstrahlung spectrum on the target.

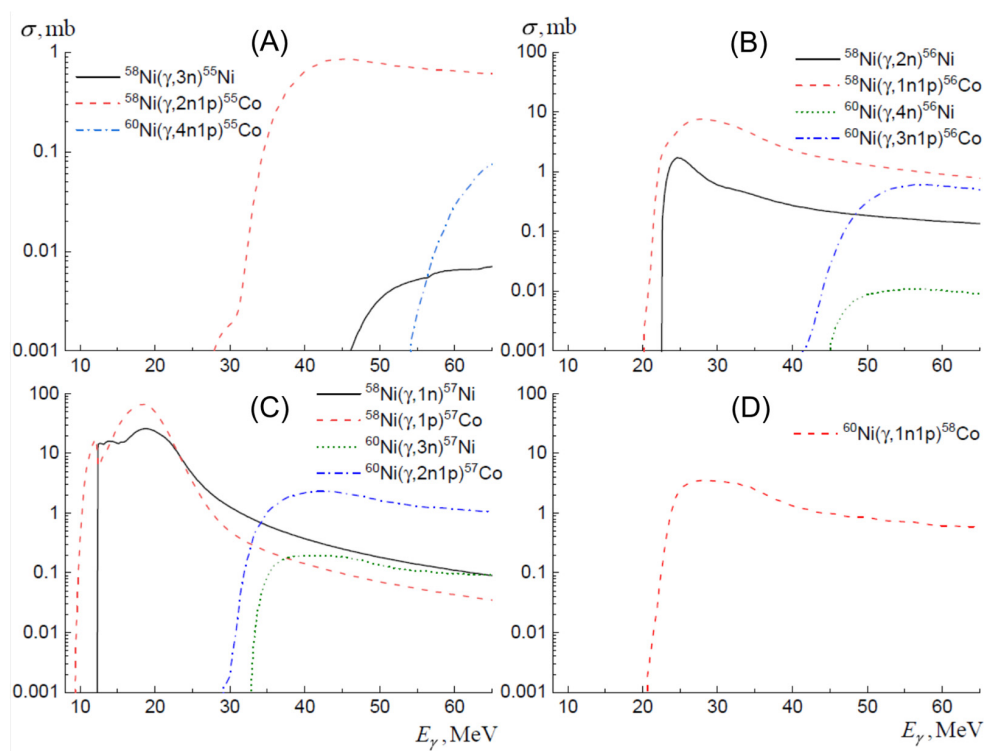


Figure 4. Calculated cross-sections of the main photonuclear reactions leading to the formation of ^{55}Co and ^{55}Ni (A), ^{56}Co and ^{56}Ni (B), ^{57}Co and ^{57}Ni (C), and ^{58}Co (D).

The bremsstrahlung spectrum calculated using a full 3D simulation of the irradiation process using the Geant4 program, taking into account the formation of gamma-quanta both in the converter and in the target, is presented on Figure 5.

3.2. Irradiation of Targets and Determination of Yields of Photonuclear Reactions

To study the yields of photonuclear reactions on nickel nuclei, two targets were irradiated in RTM-55 microtron with maximum energy of electron beam being 55 MeV [31]. The first target was a plate made of $^{\text{nat}}\text{Ni}$ with the size of 1 cm \times 1 cm, thickness of 500 μm , and weight of 440 mg. Purity of $^{\text{nat}}\text{Ni}$ was determined in our work by atomic emission spectroscopy using Thermo Scientific ICAP-6500 Duo (Horsham and Loughborough, England) and was 99.78%. The second target made of ^{60}Ni purchased from Federal State Unitary Enterprise Combine “Elektrokhimpribor” (Lesnoy, Russia) was thin trapezoidal foil 67 μm thick and with a weight of 86.5 mg. Isotope composition of ^{60}Ni -target is presented in Table 2, purity of ^{60}Ni —99.9224% according to manufacturer’s data. Tungsten plates 1 mm thick were used as converters. Monitor targets were a 0.11 mm thick cobalt plates and were located directly after the targets for irradiation. Bremsstrahlung targets, nickel targets, and monitor targets were fully overlapping the beam. Current fluctuations during the irradiations were measured using Faraday cup. Normalization of current was carried out by the processing of bremsstrahlung spectrum and by comparing experimentally measured yield of $^{59}\text{Co}(\gamma, n)^{58}\text{Co}$ reaction to the yield calculated using known cross-sections. The duration of irradiation of each target was 1 h, average currents were 73 and 48 nA for $^{\text{nat}}\text{Ni}$ and ^{60}Ni accordingly.

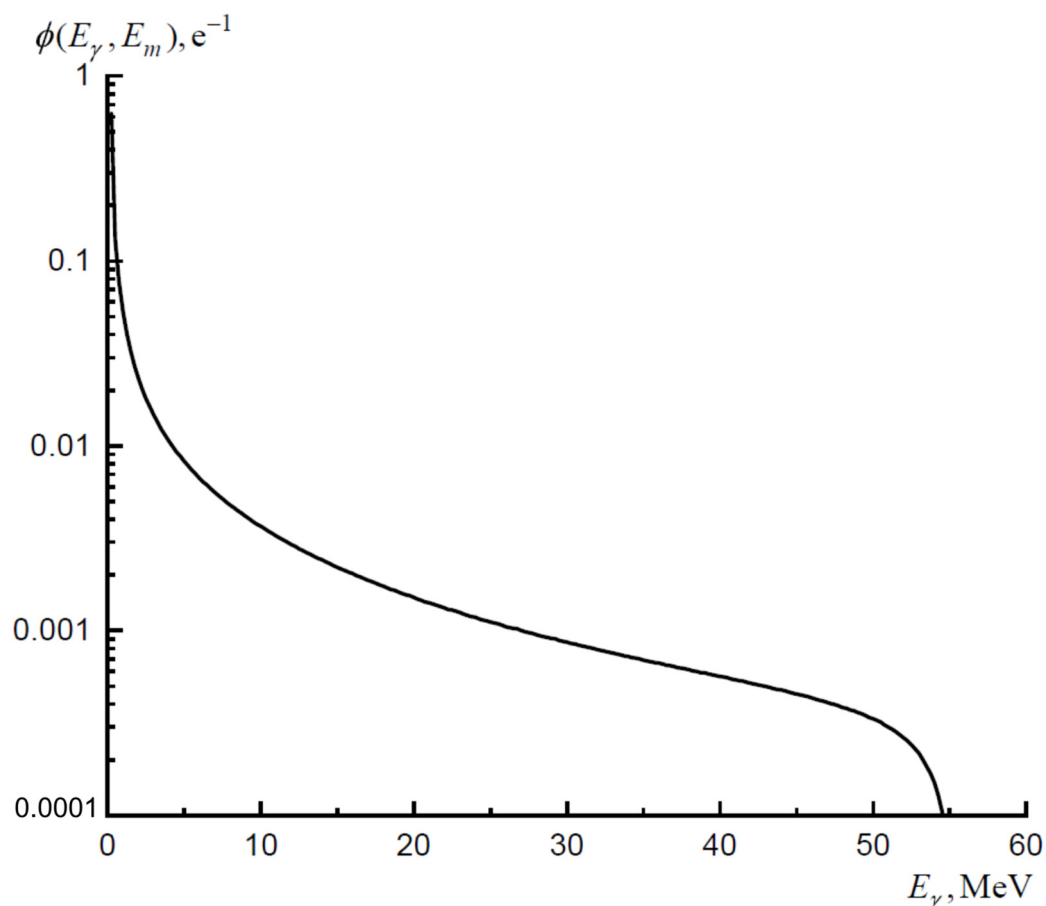


Figure 5. Bremsstrahlung spectrum per one beam electron for used converters.

Table 2. Isotope composition of ^{60}Ni foil according to manufacturer's data.

Isotope	Content, %
^{58}Ni	0.31
^{60}Ni	99.6 ± 0.1
^{61}Ni	0.05
^{62}Ni	0.04
^{64}Ni	<0.05

The residual activity of nickel targets after irradiation was registered using gamma-ray spectrometer with high-purity germanium detector GC3019 (Canberra Ind, Meridan, CT, USA). Relative efficiency of detector was 30%, energy resolution of detector was 0.9 keV for 122 keV and 1.9 keV for 1.33 MeV. Efficiency calibration of spectrometer was conducted using measurements of activity of certified point sources (^{152}Eu , ^{137}Cs , ^{60}Co , ^{241}Am) in different location geometries of source and detector and was also modeled in GEANT4. The selection of the peak maximum in the spectra was carried out using an automatic system for registration and analysis of spectra specially designed for this purpose. Spectra with the duration of 3.5 s each were saved into the database, and the analysis system allowed us to summarize them and display the total spectrum with assigned duration [32]. Activity and yields of the produced isotopes were determined using areas of the most intensive peaks corresponding to the decay of the resulting isotope in spectra of residual activity, taking into account duration of irradiation, duration of transportation and registration of spectrum, and also efficiency of gamma-quanta registration and quantum yield of gamma-transition. Gamma-spectra of each irradiated target were registered three times for 2 days during the 2 months to exactly determine both short-lived and long-lived isotopes.

Yields of photonuclear reactions on ^{nat}Ni and ^{60}Ni in $\text{kBq}/(\mu\text{A}\cdot\text{h}\cdot\text{g}/\text{cm}^2)$, normalized by electron beam charge and surface density of the target, were calculated using Equation (2):

$$Y = \frac{\lambda S}{Ck\rho(e^{-\lambda(t_3-t_1)} - e^{-\lambda(t_2-t_1)})} \quad (2)$$

where S is the area of photopeak in spectra of residual activity, corresponding to the gamma-transition during the decay of the resulting nucleus, occurring during the registration, t_1 is the irradiation time, t_2 is the starting time of the registration, t_3 is the ending time of the registration, λ is the exponential decay constant, k is the coefficient equal to the multiplication of detector efficiency, coefficient of cascade summation, and quantum yield of gamma-quant during gamma-transition, ρ is the target surface area, and C is the coefficient taking into account the change in accelerator current during the irradiation (Equation (3), Figure 6).

$$C = \int_0^{t_1} I(t)e^{-\lambda t} dt \quad (3)$$

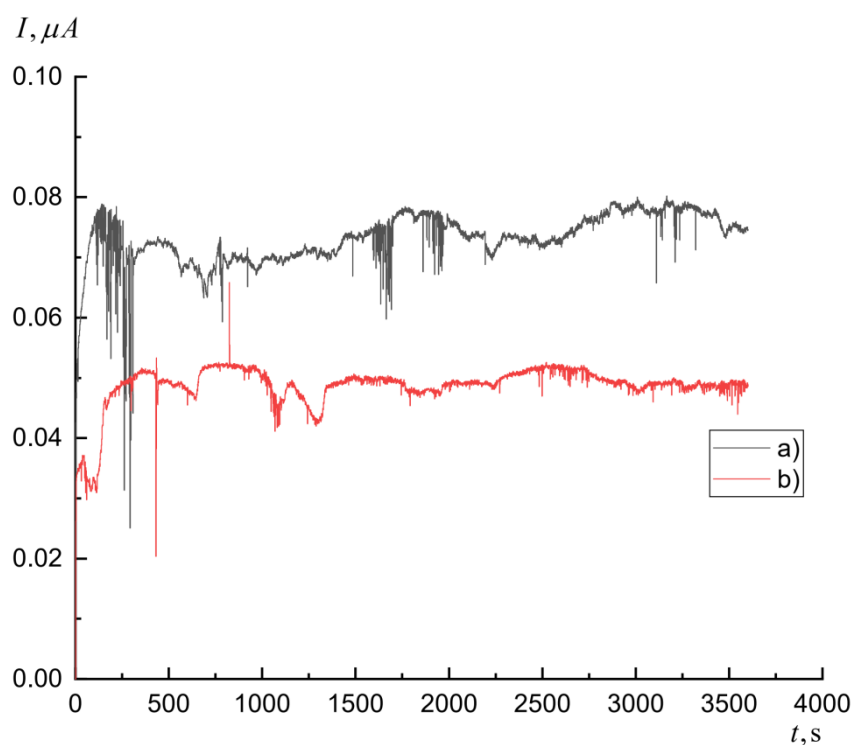


Figure 6. Accelerator current during irradiation of ^{nat}Ni (a) and ^{60}Ni (b).

Yields of reactions on ^{58}Ni were calculated as a difference between the yields of isotope production on natural mix and on ^{60}Ni , taking into account the percentage of ^{58}Ni and ^{60}Ni in natural mix. The accuracy of the selected calculation method was confirmed by the ratio of formation yields after the irradiation of ^{60}Ni and ^{nat}Ni (3.85 ± 0.05) coincided within the margin of error with the ratio of ^{60}Ni content in targets—3.81.

3.3. Separation of Co(II) Isotopes from Irradiated Nickel Target

DGA resin Normal (base-N,N,N',N'-tetraoctyl-1,5-diglycolamide, particle size 100–150 μm , TrisKem Int., Bruz, France) was used for separation. This resin sorbs Co(II) in solutions of HCl with concentration more than 6 M [33]. In these solutions, the distribution coefficient (K_d) for Co(II) reaches 20, while $K_d(\text{Ni})$ does not exceed 1 in solutions of HCl with concentration less than 10 M, which allows one to separate Co(II) and Ni(II) using this sorbent. $K_d(\text{Co})$ decreases with quantity of HCl decreasing: in a more diluted solution of HCl, i.e., less than 4 M, Co(II) is not retained on the column.

To optimize the separation method of carrier-free Co(II) from irradiated nickel, experiments with the plate made of ^{nat}Ni (1 cm \times 1 cm), similar to the plate from Section 3.2 were carried out. The irradiated plate was dissolved in 12 M HCl by prolonged heating, then the solution was evaporated to dryness in 9 M HCl. The sorbent was preliminarily held in 0.001 M HCl for 1 h, then the column (height 4 cm, diameter 0.6 cm, volume 2 mL) was filled with it. After the dissolution of the irradiated target, 0.5–1 mL of obtained solution was placed in the column with DGA resin; Co(II), unlike Ni(II), was sorbed onto the column. The remaining Ni(II) was eluted with 5 mL of 9 M HCl, then Co(II) was eluted with 5 mL of HCl solution with the concentration varying from 0.01 M to 3 M. Fractions of 1 mL were collected during the separation, the content of Co(II) and Ni(II) was determined using gamma-spectroscopy with high-purity germanium detector GC1020 (Canberra Ind.). Co(II) was identified by peaks of ^{57}Co (122 keV, 85.6%), and Ni(II) was identified by peaks of ^{57}Ni (127 keV, 16.7%) and ^{56}Ni (158 keV, 98.8%).

4. Conclusions

Targets made of ^{nat}Ni and ^{60}Ni were irradiated by bremsstrahlung photons with energy up to 55 MeV; the radionuclide composition and yields of nuclear reactions on ^{nat}Ni , ^{60}Ni , and ^{58}Ni were determined. It was established that in every case, the activities of produced $^{56,57,58}\text{Co}$ were higher than the activity of ^{55}Co , and therefore enough for preclinical research of radiopharmaceuticals based on cobalt. It was also demonstrated that the radionuclide purity of ^{55}Co produced by the photonuclear method at 55 MeV is not sufficient for PET. A fast, simple, and effective method of cobalt isotopes separation without a carrier from irradiated targets by extraction chromatography was developed; it was demonstrated that the separation of Co(II) is possible in wide range of HCl concentrations (from 0.01 to 3 M). The separation factor of Ni/Co was $2.8 \cdot 10^5$, the yield of Co(II) was close to quantitative, and separation lasted for no longer than 0.5 h.

Author Contributions: Conceptualization, A.G.K., A.A.K., S.E.V. and B.F.M.; methodology, A.G.K., S.S.B., V.V.K. and A.A.K.; software, S.S.B. and A.A.K.; validation, A.G.K., A.A.K., S.E.V. and B.F.M.; formal analysis, A.G.K., S.S.B. and A.A.K.; investigation, A.G.K., J.S.B., T.Y.E., S.S.B., A.A.K. and V.V.K.; resources, V.V.K., S.E.V. and B.F.M.; data curation, S.S.B.; writing—original draft preparation, A.G.K., J.S.B. and T.Y.E.; writing—review and editing, S.S.B., A.A.K., S.E.V. and B.F.M.; visualization, A.G.K., J.S.B., T.Y.E., S.S.B. and A.A.K.; supervision, B.F.M.; project administration, B.F.M.; funding acquisition, A.G.K., S.E.V. and B.F.M. All authors have read and agreed to the published version of the manuscript.

Funding: The study was supported by the Russian Science Foundation (project no. 21-13-00449).

Institutional Review Board Statement: Not applicable.

Informed Consent Statement: Not applicable.

Data Availability Statement: Not applicable.

Conflicts of Interest: The authors declare no conflict of interest.

References

1. Kazakov, A.G.; Ekatova, T.Y.; Babenya, J.S. Photonuclear production of medical radiometals: A review of experimental studies. *J. Radioanal. Nucl. Chem.* **2021**, *328*, 493–505. [[CrossRef](#)]
2. Lagunas-Solar, M.C.; Jungerman, J.A. Cyclotron production of carrier-free cobalt-55, a new positron-emitting label for bleomycin. *Int. J. Appl. Radiat. Isot.* **1979**, *30*, 25–32. [[CrossRef](#)]
3. Nieweg, O.E.; Beekhuis, H.; Paans, A.M.J.; Piers, D.A.; Vaalburg, W.; Welleweerd, J.; Wiegman, I.; Woldring, M.G. Detection of lung cancer with ^{55}Co -bleomycin using a positron camera. A comparison with ^{57}Co -bleomycin and ^{55}Co -bleomycin single photon scintigraphy. *Eur. J. Nucl. Med.* **1982**, *7*, 104–107. [[CrossRef](#)] [[PubMed](#)]
4. Sharma, H.; Zweit, J.; Smith, A.M.; Downey, S. Production of cobalt-55, a short-lived, positron emitting radiolabel for bleomycin. *Int. J. Radiat. Appl. Instrumentation. Part A* **1986**, *37*, 105–109. [[CrossRef](#)]
5. Goethals, P.; Volckaert, A.; Vandewielle, C.; Dierckx, R.; Lameire, N. ^{55}Co -EDTA for renal imaging using positron emission tomography (PET): A feasibility study. *Nucl. Med. Biol.* **2000**, *27*, 77–81. [[CrossRef](#)]

6. Andersen, T.L.; Baun, C.; Olsen, B.B.; Dam, J.H.; Thisgaard, H. Improving contrast and detectability: Imaging with [⁵⁵Co]Co-DOTATATE in comparison with [⁶⁴Cu]Cu-DOTATATE and [⁶⁸Ga]Ga-DOTATATE. *J. Nucl. Med.* **2020**, *61*, 228–235. [[CrossRef](#)] [[PubMed](#)]
7. Dam, J.H.; Olsen, B.B.; Baun, C.; Høiland-Carlsen, P.F.; Thisgaard, H. A PSMA ligand labeled with cobalt-55 for PET imaging of prostate cancer. *Mol. Imaging Biol.* **2017**, *19*, 915–922. [[CrossRef](#)] [[PubMed](#)]
8. Zhou, Y.; Baidoo, K.E.; Brechbiel, M.W. Mapping biological behaviors by application of longer-lived positron emitting radionuclides. *Adv. Drug Deliv. Rev.* **2013**, *65*, 1098–1111. [[CrossRef](#)] [[PubMed](#)]
9. Blower, P.J. A nuclear chocolate box: The periodic table of nuclear medicine. *Dalt. Trans.* **2015**, *44*, 4819–4844. [[CrossRef](#)]
10. Radford, L.L.; Fernandez, S.; Beacham, R.; El Sayed, R.; Farkas, R.; Benešová, M.; Müller, C.; Lapi, S.E. New ⁵⁵Co-labeled albumin-binding folate derivatives as potential PET agents for folate receptor imaging. *Pharmaceuticals* **2019**, *12*, 166. [[CrossRef](#)]
11. Jansen, H.M.L.; Knollema, S.; Van Der Duin, L.V.; Willemsen, A.T.M.; Wiersma, A.; Franssen, E.J.F.; Russel, F.G.M.; Korf, J.; Paans, A.M.J. Pharmacokinetics and dosimetry of cobalt-55 and cobalt-57. *J. Nucl. Med.* **1996**, *37*, 2082–2086.
12. Stevens, H.; Jansen, H.M.L.; De Reuck, J.; Lemmerling, M.; Strijckmans, K.; Goethals, P.; Lemahieu, I.; De Jong, B.M.; Willemsen, A.T.M.; Korf, J. ⁵⁵Cobalt (Co) as a PET-tracer in stroke, compared with blood flow, oxygen metabolism, blood volume and gadolinium-MRI. *J. Neurol. Sci.* **1999**, *171*, 11–18. [[CrossRef](#)]
13. Jansen, H.M.L.; Van Der Naalt, J.; Van Zomeren, A.H.; Paans, A.M.J.; Veenma-van Der Duin, L.; Hew, J.M.; Pruim, J.; Minderhoud, J.M.; Korf, J. Cobalt-55 positron emission tomography in traumatic brain injury: A pilot study. *J. Neurol. Neurosurg. Psychiatry* **1996**, *60*, 221–224. [[CrossRef](#)] [[PubMed](#)]
14. Heppeler, A.; André, J.P.; Buschmann, I.; Wang, X.; Reubi, J.C.; Hennig, M.; Kaden, T.A.; Maecke, H.R. Metal-ion-dependent biological properties of a chelator-derived somatostatin analogue for tumour targeting. *Chem. A Eur. J.* **2008**, *14*, 3026–3034. [[CrossRef](#)]
15. Amjed, N.; Hussain, M.; Aslam, M.N.; Tárkányi, F.; Qaim, S.M. Evaluation of nuclear reaction cross sections for optimization of production of the emerging diagnostic radionuclide ⁵⁵Co. *Appl. Radiat. Isot.* **2016**, *108*, 38–48. [[CrossRef](#)]
16. Sitarz, M.; Cussonneau, J.P.; Matulewicz, T.; Haddad, F. Radionuclide candidates for β+γ coincidence PET: An overview. *Appl. Radiat. Isot.* **2020**, *155*, 108898. [[CrossRef](#)]
17. Zaman, M.; Kim, G.; Naik, H.; Kim, K.; Shahid, M.; Nadeem, M.; Shin, S.G.; Cho, M.H. Flux weighted average cross-sections of ^{nat}Ni(γ,x) reactions with the bremsstrahlung end-point energies of 55, 59, 61 and 65 MeV. *Nucl. Phys. A* **2018**, *978*, 173–186. [[CrossRef](#)]
18. Naik, H.; Kim, G.; Nguyen, T.H.; Kim, K.; Shin, S.G.; Kye, Y.C.M. Measurement of ^{nat}Ni(γ,xn)^{57,56}Ni and ^{nat}Ni(γ,pxn)^{58–55}Co reaction cross sections in bremsstrahlung with end-point energies of 65 and 75 MeV. *J. Radioanal. Nucl. Chem.* **2020**, *324*, 837–846. [[CrossRef](#)]
19. Mazière, B.; Stulzaft, O.; Verret, J.; Comar, D.; Syrota, A. [⁵⁵Co]- and [⁶⁴Cu]-DTPA: New radiopharmaceuticals for quantitative tomocisternography. *Int. J. Appl. Radiat. Isot.* **1983**, *34*, 595–601. [[CrossRef](#)]
20. Spellerberg, S.; Reimer, P.; Blessing, G.; Coenen, H.H.; Qaim, S.M. Production of ⁵⁵Co and ⁵⁷Co via proton induced reactions on highly enriched ⁵⁸Ni. *Appl. Radiat. Isot.* **1998**, *49*, 1519–1522. [[CrossRef](#)]
21. Jalilian, A.R.; Rowshanfarzad, P.; Akhlaghi, M.; Sabet, M.; Kamali-Dehghan, M.; Pouladi, M. Preparation and biological evaluation of a [⁵⁵Co]-2-acetylpyridine thiosemicarbazone. *Sci. Pharm.* **2009**, *77*, 567–578. [[CrossRef](#)]
22. Jalilian, A.R.; Rowshanfarzad, P.; Yari-Kamrani, Y.; Sabet, M.; Majdabadi, A. Preparation and evaluation of [⁵⁵Co](II)-DTPA for blood cell labeling. *Open Inorg. Chem. J.* **2009**, *3*, 21–25. [[CrossRef](#)]
23. Valdovinos, H.F.; Graves, S.; Barnhart, T.; Nickles, R.J. ⁵⁵Co separation from proton irradiated metallic nickel. *AIP Conf. Proc.* **2014**, *1626*, 217–220. [[CrossRef](#)]
24. Reimer, P.; Qaim, Q.S. Excitation functions of proton induced reactions on highly enriched ⁵⁸Ni with special relevance to the production of ⁵⁵Co and ⁵⁷Co. *Radiochim. Acta* **1998**, *80*, 113–120. [[CrossRef](#)]
25. Mastren, T.; Marquez, B.V.; Sultan, D.E.; Bollinger, E.; Eisenbeis, P.; Voller, T.; Lapi, S.E. Cyclotron production of high-specific activity ⁵⁵Co and in vivo evaluation of the stability of ⁵⁵Co metal-chelate-peptide complexes. *Mol. Imaging* **2015**, *14*, 526–532. [[CrossRef](#)]
26. Mastren, T.; Sultan, D.; Lapi, S.E. Production and separation of ⁵⁵Co via the ⁵⁸Ni(p,α)⁵⁵Co reaction. *AIP Conf. Proc.* **2012**, *1509*, 96–100. [[CrossRef](#)]
27. Valdovinos, H.F.; Hernandez, R.; Graves, S.; Ellison, P.A.; Barnhart, T.E.; Theuer, C.P.; Engle, J.W.; Cai, W.; Nickles, R.J. Cyclotron production and radiochemical separation of ⁵⁵Co and ^{58m}Co from ⁵⁴Fe, ⁵⁸Ni and ⁵⁷Fe targets. *Appl. Radiat. Isot.* **2017**, *130*, 90–101. [[CrossRef](#)]
28. Valdovinos, H.F.; Graves, S.; Barnhart, T.; Nickles, R.J. Simplified and reproducible radiochemical separations for the production of high specific activity ⁶¹Cu, ⁶⁴Cu, ⁸⁶Y and ⁵⁵Co. *AIP Conf. Proc.* **2017**, *1845*, 020021. [[CrossRef](#)]
29. Koning, A.J.; Duijvestijn, M.C.; Hilarie, S. Talys 1.0. In Proceedings of the International Conference on Nuclear Data for Science and Technology, Nice, France, 17 June 2007; pp. 211–214.
30. Belgya, T.; Bersillon, O.; Capote, R.; Fukahori, T.; Zhigang, G.; Goriely, S.; Herman, M.; Ignatyuk, A.V.; Kailas, S.; Koning, A.; et al. *Handbook for Calculations of Nuclear Reaction Data, RIPL-2*; IAEA-TECDOC-1506; IAEA: Vienna, Austria, 2006. Available online: <http://www-nds.iaea.org/RIPL-2/> (accessed on 20 January 2022).

31. Ermakov, A.N.; Ishkhanov, B.S.; Kamanin, A.N.; Pakhomov, N.I.; Khankin, V.V.; Shvedunov, V.I.; Shvedunov, N.V.; Zhuravlev, E.E.; Karev, A.I.; Sobenin, N.P. A multipurpose pulse race-track microtron with an energy of 55 MeV. *Instrum. Exp. Tech.* **2018**, *61*, 173–191. [[CrossRef](#)]
32. Belyshev, S.S.; Stopani, K.A. Automatic data acquisition and analysis in activation experiments. *Mosc. Univ. Phys. Bull.* **2013**, *68*, 88–91. [[CrossRef](#)]
33. Pourmand, A.; Dauphas, N. Distribution coefficients of 60 elements on TODGA resin: Application to Ca, Lu, Hf, U and Th isotope geochemistry. *Talanta* **2010**, *81*, 741–753. [[CrossRef](#)]